



Dupuytren's disease susceptibility gene, *EPDR1*, is involved in myofibroblast contractility



Kim A. Staats^a, Timothy Wu^a, Bing S. Gan^{b,c}, David B. O'Gorman^{b,c}, Roel A. Ophoff^{a,d,e,*}

^a Center for Neurobehavioral Genetics, Semel Institute for Neuroscience and Human Behavior, University of California Los Angeles, CA, USA

^b Department of Surgery, University of Western Ontario, St Joseph's Health Centre, London, Ontario, Canada

^c Cell and Molecular Biology Laboratory, Hand and Upper Limb Centre, London, Ontario, Canada

^d Department of Human Genetics, David Geffen School of Medicine, University of California Los Angeles, CA, USA

^e Brain Center Rudolf Magnus, Department of Psychiatry, University Medical Center Utrecht, The Netherlands

ARTICLE INFO

Article history:

Received 6 January 2016

Received in revised form 1 April 2016

Accepted 28 April 2016

Keywords:

Genetics

GWAS

Dupuytren's contracture

Ependymin

FPCL

ABSTRACT

Background: Dupuytren's Disease is a common disorder of the connective tissue characterized by progressive and irreversible fibroblastic proliferation affecting the palmar fascia. Progressive flexion deformity appears over several months or years and although usually painless, it can result in a serious handicap causing loss of manual dexterity. There is no cure for the disease and the etiology is largely unknown. A genome-wide association study of Dupuytren's Disease identified nine susceptibility loci with the strongest genetic signal located in an intron of *EPDR1*, the gene encoding the Ependymin Related 1 protein.

Objective: Here, we investigate the role of *EPDR1* in Dupuytren's Disease.

Methods: We research the role of *EPDR1* by assessing gene expression in patient tissue and by gene silencing in fibroblast-populated collagen lattice (FPCL) assay, which is used as an in vitro model of Dupuytren's contractures.

Results: The three alternative transcripts produced by the *EPDR1* gene are all detected in affected Dupuytren's tissue and control unaffected palmar fascia tissue. Dupuytren's tissue also contracts more in the FPCL paradigm. Dicer-substrate RNA-mediated knockdown of *EPDR1* results in moderate late stage attenuation of contraction rate in FPCL, implying a role in matrix contraction.

Conclusion: Our results suggest functional involvement of *EPDR1* in the etiology of Dupuytren's Disease.

© 2016 Published by Elsevier Ireland Ltd on behalf of Japanese Society for Investigative Dermatology.

1. Introduction

Dupuytren's Disease (Dupuytren) or Dupuytren's Contracture (OMIM: 126900) is a common disorder of the connective tissue characterized by progressive and irreversible fibroblastic proliferation affecting the palmar fascia. Shortening of the thickened palmar fascia results in progressive digital flexion deformity. The earliest sign of Dupuytren is the formation of fibrous nodules in the palm. Progressive flexion deformity may appear over several months or years, typically affecting the ring finger and the little finger [1]. Dupuytren is often bilateral and, although usually painless, it can result in a serious handicap causing loss of manual dexterity and the inability to touch, stroke, or shake hands in a normal manner. The average age of onset is 60

years and the incidence increases with increasing years. Standard treatment consists of surgical excision of pathologic nodules and cords or percutaneous division but other treatment modalities are emerging [2–4]. However, there is no cure for the disease, the origin of the disease is largely unknown, and there is a high recurrence rate after surgery [5,6].

The reported prevalence of Dupuytren varies between 0.2% and 56% depending on methods used [7,8]. A clinic-based study highlighted the gender differences of the disease with a fourfold male preponderance, especially for those with a relatively early onset (age <45 years) or for patients treated surgically [9]. The sex difference in prevalence diminishes with increasing age. In the UK, the incidence of new consultations with a family physician for Dupuytren is 34/100,000 men annually [10].

The histological and biochemical alterations in Dupuytren-affected tissue are similar to those in the active stages of connective tissue wound repair; high numbers of fibroblasts, increased deposition of extracellular matrix proteins (especially collagen) and the presence of contractile myofibroblasts. The latter

* Corresponding author at: Center for Neurobehavioral Genetics, Semel Institute for Neuroscience and Human Behavior, University of California Los Angeles, California, USA.

E-mail address: Ophoff@ucla.edu (R.A. Ophoff).

is a population of cells involved in the granulation stage of wound healing responsible for wound contraction [11], and are recognized by α -smooth muscle actin (α -SMA) expression. The expression of α -SMA can be increased by Transforming Growth Factor, Beta 1 (TGF β 1), by stimulating the conversion of fibroblasts to myofibroblasts [12–14]. Histological analysis of disease tissue shows a corresponding decrease in the amount of type III collagen as a percentage of the total collagen with disease progression [15]. To measure the contractility of (myo)fibroblasts, fibroblast-populated collagen lattice (FPCL) contraction assays are used in functional Dupuytren research [16–19] to assess the contractility of fibroblasts to particular stimuli, including inflammatory cues [20]. Despite these efforts, the pathophysiological basis of Dupuytren is incompletely understood.

A genome-wide association study (GWAS) for Dupuytren identified nine susceptibility loci, showing robust genetic evidence with relatively high odds ratios (ranging from 0.72–1.98) compared to other complex human traits [21]. The results further implicated a potential involvement of Wnt signalling in disease and demonstrate that genetic variants play an important role in the etiology of Dupuytren in patients with European ancestry [22]. The most significant finding was at single nucleotide polymorphism (SNP) rs16879765, located in an intron of *EPDR1*, the Ependymin Related 1 gene, with $p=5.6 \times 10^{-39}$ and an odds ratio of 1.98 (CI 1.78–2.18). This finding was confirmed in an independent study [23].

Little is known about *EPDR1*. The gene encodes the Ependymin Related 1 protein, and is additionally known as *MERP1*, mammalian ependymin related protein 1, and as *UCCI*, upregulated in colorectal cancer 1. Ependymins were first described as the predominant constituent of the cerebrospinal fluid of teleost fish, such as gold fish and rainbow trout (reviewed in [24]), produced by leptomeningeal fibroblasts (reviewed in [24]). It is reported that a calcium-induced conformational change in ependymin is important for its interaction with the extracellular matrix [25], particularly by association with collagen [26,27]. It was therefore subsequently hypothesized that ependymin is essential for cell-to-cell contact as a (anti) cell adhesion molecule [25]. In humans *EPDR1* gene expression is broadly expressed throughout tissues, with a particular high expression in brain, in addition to contractile tissues, such as muscle tissue and the heart [28–30].

2. Materials and methods

2.1. Cell line collection

Primary fibroblasts derived from Dupuytren's tissue (D), normal palmar fascia tissue (PF) and control tissue (CT) were obtained at the Lawson Health Research Institute, London, Ontario Canada. We collected 4 allogeneic isolates from unrelated individuals per group. All tissues were surgically resected from patients who were undergoing primary surgery at St. Joseph's Hospital, London, Ontario, as described previously [31]. Dupuytren's cells were derived from fibrotic palmar fascia, whereas PF and CT fibroblasts were both derived from visibly unaffected, palmar fascia. PF fibroblasts are derived from the palmar fascia of an individual with Dupuytren's in an adjacent digit, whereas CT fibroblasts are from the palmar fascia of an individual with Carpal Tunnel syndrome. All of these fibroblasts are derived from the same tissue source, palmar fascia. Patient-derived tissues were cultured up to a maximum of 8 passages in all protocols. Primary human neonatal foreskin fibroblasts (PCS-201-010) were purchased from ATCC (Manassas, VA, USA) and were cultured up to 9 passages. All cells were grown in Fibroblast Basal Medium (FBM, PCS-201-030; ATCC, Manassas, VA, USA) supplemented with Fibroblast Growth kit-Low Serum (PCS-201-041; ATCC, Manassas,

VA, USA) and 10 units/mL penicillin-streptomycin (15140-122; Life Technologies, Carlsbad, CA, USA) at 37 °C and 5% (vol/vol) CO₂ in a humidified incubator.

2.2. Gene expression results from Genevar database

In order to consider genetic effects of the disease locus (SNP rs16879765) on local (*cis*) gene expression levels we used the available Genevar database version 3.3.0 [32] with the GenCord dataset [33], in which gene expression was determined by Illumina HumanWG-6 v3. We restricted our analyses to the expression data of fibroblasts (GenCord-F) as being the most-related cell type to Dupuytren affected tissue.

2.3. RNA isolation and cDNA conversion

Adherent fibroblast cultures were trypsinized, re-suspended in FBM and pelleted prior to cell lysis with buffer RLT from the RNeasy Mini Kit (74104; Qiagen, Venlo, The Netherlands). Lysed samples were homogenized with QIAshredder columns (79654; Qiagen, Venlo, The Netherlands) and stored at –80 °C or processed immediately per manufacturer's protocol. Purified RNA was quantified using the Quant-iT Ribogreen assay (R11490; Life Technologies, Carlsbad, CA, USA) and RIN values were assessed using the Agilent Bioanalyzer 2100 (G2940CA; Agilent Technologies, Santa Clara, CA, USA). Collagen gels from select FPCL experiments were suspended directly in TRIzol (15596-026; Life Technologies, Carlsbad, CA, USA) and incubated at room temperature until completely dissociated. Samples were stored at –80 °C until ready for extraction. After thawing, extraction occurred by adding 0.2x volume of chloroform to the TRIzol suspension. Samples were mixed and centrifuged at 12,000g for 15 min at 4 °C. The top aqueous phase was combined with 1 vol of 70% ethanol and loaded onto RNeasy spin columns. RNA purification with RNeasy was performed as described above. 100–250 ng of RNA for each sample was used in cDNA synthesis with the High-Capacity RNA-to-cDNA Kit (4387406; Life Technologies, Carlsbad, CA, USA) per manufacturer's protocol.

2.4. RT-PCR gene expression

EPDR1 transcript presence was assessed via RT-PCR. Custom cDNA primers were generated using the NCBI primer blast tool and subsequently synthesized by IDT DNA, (Coralville, Iowa, CA USA). The GAPDH positive control primer pair was obtained from Walker et al. [34] (forward: 5'-AATCCCATCACCATCTTCCA-3', reverse: 5'-TGGACTCCACGACGTACTCA-3'). Three *EPDR1* mRNA variants were detected by two primer pairs: pair 1 (forward: 5'-TCAGATTGACCAAGCCACCAA-3', reverse: 5'-ACGTGCTTG-GAGGGGTAAAC-3') detects mRNA variant 1 and 3, and pair 2 (forward: 5'-GATCTCAAAGCGGCAGAGG-3', reverse: 5'-CGTGCTTGAGGGG TAAACA-3') detects mRNA variant 1 and 2. Synthesized cDNA was used in conventional touchdown PCR with 1 μ M of the above primers for gene expression analysis. The PCR occurred with 1x MyFi PCR Master Mix (BIO-25049, Bio Line, London UK) and the BioRad C1000 thermocycler (185-1048, BioRad, Hercules, CA USA). Select PCR templates were treated with Exo-Sap-IT (78200, Affymetrix, Santa Clara, CA USA) and were subsequently Sanger sequenced to ensure that the proper product was detected.

2.5. Quantitative real time-PCR

Relative *EPDR1* gene expression was assessed with Primetime qPCR Assay Hs.PT.58.38898209 and Hs.PT.58.20021550 (IDT DNA, Coralville, Iowa, USA), IDT DNA Primetime qPCR assays for *GAPDH*

(Hs.PT.39a.22214836), *ACTB* (Hs.PT.39a.22214847), and *HPRT1* (Hs.PT.58.20881146) were used to normalize expression data. 2.5 ng of cDNA per sample were combined with 2x Taqman Gene Expression Master Mix (4369016; Life Technologies, Carlsbad, CA, USA), 10x Primetime qPCR assay (IDT DNA, Coralville, Iowa, USA). Samples were run in triplicate on the ABI PRISM 7900HT for 60 cycles. Cycling conditions were set as recommended by the Taqman master mix protocol. Relative gene expression was calculated with the $\Delta\Delta CT$ method and the data presented is the average when normalizing against 3 housekeeping genes (*ACTB*, *GAPDH* and *HPRT1*).

2.6. Fibroblast-populated collagen lattice (FPCL)

Contractile activity was measured with fibroblasts cultured in 2 mg/ml of rat tail collagen I (A1048301; Life Technologies, Carlsbad, CA, USA) at a density of 1.5×10^5 cells/mL. Fibroblasts were cultured in a monolayer to approximately 80% confluency, trypsin-released and re-suspended in fibroblast basal medium (FBM). Rat tail collagen was combined with cold 10x PBS and neutralizing 1 M NaOH. Combination of the collagen and cell suspension yielded a final concentration of 2 mg/ml collagen, 1.5×10^5 cells/mL, 3.5% (vol/vol) 1 M NaOH and PBS for isotonicity. The collagen-cell suspension was immediately aliquoted into 24-well tissue culture plates and allowed to polymerize at 37 °C for 20 min. An equivalent volume of culture media was then added on each lattice. Treatment in all experiments occurred 24 post seeding at the earliest. Tension was allowed to build in the collagen lattices for 48 h prior to release by running a pipette tip along the well edges. Lattice release is $t = 0$. Recombinant human TGF β 1 (GF111, Millipore, Billerica, MA, USA) was applied 1 h before lattice release (47 h post seeding). Lyophilized TGF β 1 was re-suspended in Hyclone water to make a 0.5 mg/ml stock and subsequently diluted in FBM to generate a 10 ng/ml working stock. Media was aspirated prior to applying the TGF β 1 solution. Plates were imaged at a fixed distance using the BioRad Gel Doc XR+ System (170-8195, BioRad, Hercules, CA, USA) with white light at various time points. Gel areas were calculated using the ImageJ measuring tool, v1.47, and measured in a single-blinded fashion.

2.7. Cell counts

Cell counts were performed with adherent cultures to assess proliferation in different conditions. Adherent cultures in 24 well plates were re-suspended in FBM as described above at various time points. Aliquots of re-suspended cells were combined with Trypan Blue (145-0003; BioRad, Hercules, CA, USA) in a 1:1 ratio and loaded onto a standard hemocytometer. Cells were counted manually using a conventional inverted microscope and only live cells were counted on tissue culture plastic.

2.8. RNA interference (RNAi)

Custom IDT DNA dicer-substrate RNA (DsiRNA) oligos were used for gene silencing. Per targeted sequence prediction HSC.RNAI.N017549.12.2 targets all three mRNA transcripts of *EPDR1*. DS NC1 (IDT DNA, Coralville, Iowa, USA) was used as a universal scrambled control in all RNAi experiments. DsiRNA ligated with TYE-563 was used to optimize transfection efficiency; transfected cells were visualized with a Texas-Red filter using fluorescent microscopy. Percent transfection was approximated by assessing the percentage of fluorescent cells in the total cell population, and found to equal or exceed 90% in all experiments. DsiRNA oligos and Lipofectamine 3000 (L3000-008; Life Technologies, Carlsbad, CA, USA) were mixed in Opti-MEM reduced serum medium (31985062; Life Technologies, Carlsbad, CA, USA) and combined

in 24-well tissue culture plates to yield a concentration of 10 nM DsiRNA per well at a volume of 1.5 μ l Lipofectamine 3000 per well. Knockdown efficiency was initially evaluated using monolayer cultures in 24-well plates. Cells were seeded at 2×10^4 cells/mL and treated with DsiRNAs per above protocol at 24 h post seeding. In FPCL experiments, DsiRNAs were applied at 24 and 47 h post seeding. The above concentrations of DsiRNA and Lipofectamine 3000 were maintained throughout the experiments. Half volume of reagents was applied at 24 h post seeding while an equimolar half was applied at 47 h post seeding; rhTGF β 1 was applied along the second half in applicable conditions.

2.9. Statistics

Analysis was performed with the statistical software package Prism Origin 6.0c (GraphPad Software, La Jolla, USA). A two-way ANOVA for repeated measures was used for assessing the contraction over time with a Sidak posthoc analysis restricted to the differences a time point across groups. Significance threshold was set at $p < 0.05$. In graphs means are depicted and error bars represent the standard deviation.

3. Results

To understand the role of the Dupuytren-associated SNP rs16879765, we first confirmed that the associated haplotype is restricted to the *EPDR1* gene and does not include other protein coding genes [21]. Since the disease locus may represent a regulatory element of a distant protein coding gene, we first examined the available gene expression data with Genevar [32] from cells derived from umbilical cords of 75 Geneva GenCord individuals [33], which is a publicly available dataset. We specifically focused on the analysis of gene expression of fibroblasts, as this cell type is involved in fibrosis observed in Dupuytren and as regulation of gene expression may be cell type specific [33]. This analysis shows that carriers of the minor allele (A/G) have an increased expression of *EPDR1* compared to individuals carrying the major allele only (G/G; empirical $p = 0.03$, Fig. 1). There were no individuals available within this dataset homozygous for the minor allele. Additionally, rs16879765 is not correlated with an altered gene expression of the neighboring gene *SPFR4* in this dataset.

To confirm that *EPDR1* may contribute to Dupuytren pathophysiology, we tested whether *EPDR1* mRNA transcripts are detected in affected Dupuytren and control tissue. Each mRNA transcript of *EPDR1* (Fig. 2A) was successfully amplified in affected

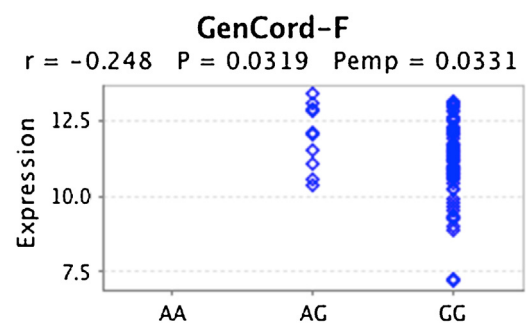


Fig. 1. The Dupuytren-associated SNP rs16879765 influences *EPDR1*. *EPDR1* gene expression of fibroblasts from individuals from the GenCord dataset [33] heterozygous for the minor allele (A/G) compared to those homozygous for the major allele (G/G; linear regression correlation coefficient after 10,000 permutations by Genevar). The used software GeneVar does not assess strandedness of variants and therefore the alleles G and A described here correspond to C and T, respectively.

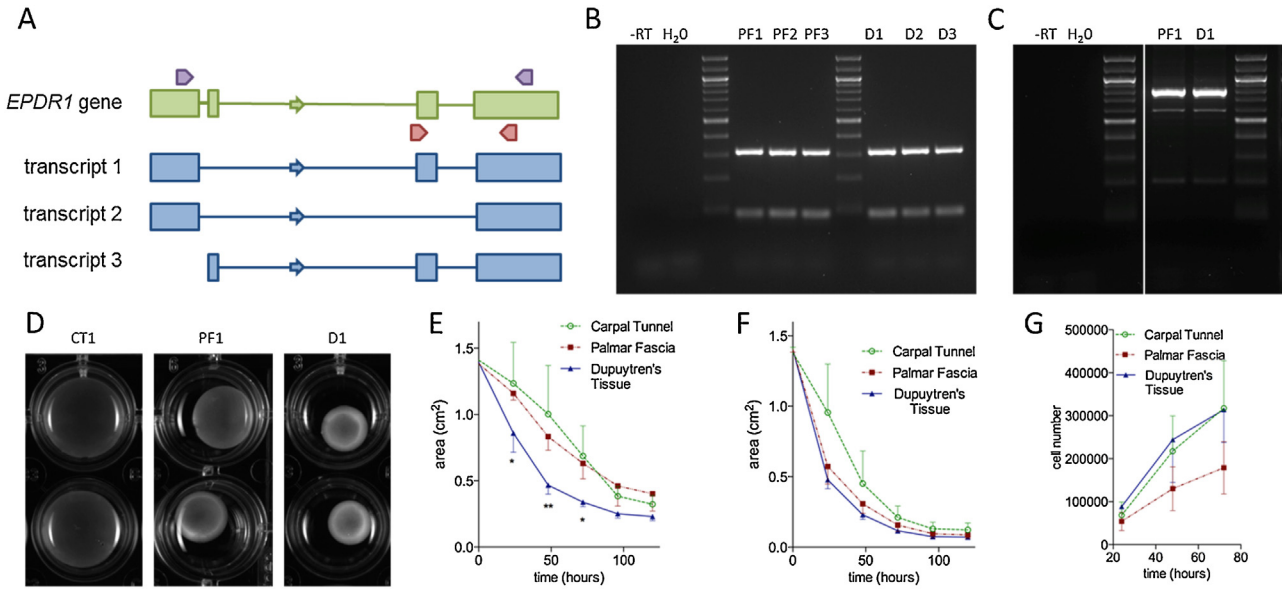


Fig. 2. Dupuytren's affected tissue expresses EPDR1 and models Dupuytren's contraction *in vitro*. A. PCR approach to detect each of three EPDR1 transcripts. The primer set depicted in red amplifies transcript 1 and 3. The purple primer set amplifies transcript 1 and 2. B. PCR product of EPDR1 transcripts 1 and 3 (amplicon 317 bp) in different control palmar fascia fibroblast cell lines (PF1-3) and fibroblasts cell lines from affected Dupuytren's tissue (D1-3). Negative controls are negative reverse transcriptase PCR (-RT) and non template control (H₂O). Positive control is a GAPDH amplicon included in the reaction (amplicon 81 bp). Full image in Fig. S1A. C. PCR product of EPDR1 transcripts 1 (amplicon 791 bp) and 2 (amplicon 582 bp) in different control palmar fascia fibroblast cell lines (PF1-3) and fibroblasts cell lines from affected Dupuytren's tissue (D1-3). Negative controls are negative reverse transcriptase PCR (-RT) and non template control (H₂O). Transcript 2 was only obtainable when removing the positive control (GAPDH) from the reaction. Full image in Fig. S1B. D. FPCL images after 48 h without TGFβ1 stimulation from fibroblasts from palmar fascia from affected Dupuytren's tissue (D1), from control palmar fascia from the same individual as the Dupuytren's tissue (PF1) and palmar fascia from an individual with Carpal Tunnel syndrome (CT1). Full image in Fig. S2A. E. Contraction rate of fibroblast lines from carpal tunnel (n = 4), palmar fascia (n = 4) and Dupuytren's tissue (n = 4; 2-way anova with repeated measures, Sidak post hoc analysis). F. Contraction rate of fibroblast lines from carpal tunnel (n = 4), palmar fascia (n = 4) and Dupuytren's tissue (n = 4) upon TGFβ1 (10 ng/ml) stimulation (2-way anova with repeated measures, Sidak post hoc analysis). G. Cell proliferation rate of fibroblasts from carpal tunnel (n = 4), palmar fascia (n = 4) and Dupuytren's tissue on tissue culture plastic (n = 4; 2-way anova with repeated measures, Sidak post hoc analysis of means per treatment per time point). Mean ± standard deviation. *p < 0.05, **p < 0.01. (For interpretation of the references to colour in this figure legend, the reader is referred to the web version of this article.)

Dupuytren tissue, control palmar fascia and control carpal tunnel fibroblasts (Fig. 2B and C, full image in Fig. S1A and B). A sample from each transcript was subsequently Sanger sequenced confirming the accurately sized amplicon was indeed from EPDR1 (data not shown). To assess whether the fibroblast-populated collagen lattice (FPCL) assay would be a suitable model in our hands and to subsequently compare with a commercially available cell-line, we tested the rate of contraction of fibroblasts obtained

from affected Dupuytren tissue, control palmar fascia and control carpal tunnel in FPCL. With this approach we measure the contractility of fibroblasts residing in a collagen lattice, as determined by the area of the lattice (Fig. 2D, full image in Fig. S2A and B). Fibroblasts obtained from affected Dupuytren tissue contracted faster than fibroblasts from control palmar fascia (from the same individual) or from unaffected tissue from patients with carpal tunnel syndrome (different individual;

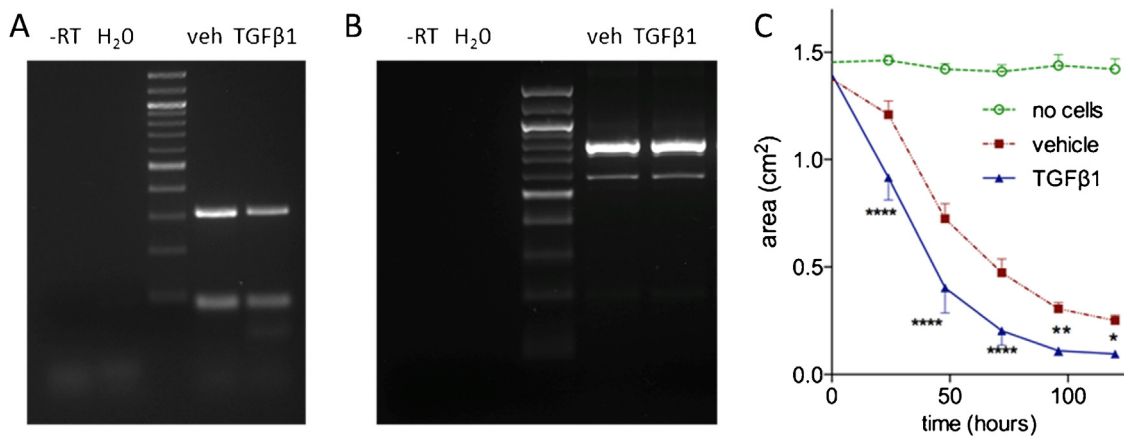


Fig. 3. Neonatal fibroblast cell line is a similarly suitable model. A. PCR product of EPDR1 transcripts 1 and 3 (amplicon 317 bp) in cell line PCS-201-010 treated by vehicle (veh) and TGFβ1 (10 ng/ml). Negative controls are negative reverse transcriptase PCR (-RT) and non template control (H₂O). Positive control is a GAPDH amplicon included in the reaction (amplicon 81 bp). Full image in Fig. S1A. B. PCR product of EPDR1 transcripts 1 (amplicon 791 bp) and 2 (amplicon 582 bp) in cell line PCS-201-010 treated by vehicle (veh) and TGFβ1 (10 ng/ml). Negative controls are negative reverse transcriptase PCR (-RT) and non template control (H₂O). Transcript 2 was only obtainable when removing the positive control (GAPDH) from the reaction. Full image in Fig. S1B. C. Contraction rate of PCS-201-010 treated with vehicle (n = 3) or 10 ng/ml TGFβ1 (n = 3; 2-way anova with repeated measures, Sidak post hoc analysis of means per treatment per time point). Lattices without cells were assessed to illustrate possible effects of dehydration on the lattices over time, but were not included in the analysis. Mean ± standard deviation. *p < 0.05, **p < 0.01, ****p < 0.0001.

Fig. 2E), consistent with previous studies. Stimulation of fibroblasts with TGF β 1 allows for increased conversion to myofibroblasts and contraction [12–14]. As expected, upon TGF β 1 application all samples contracted faster, with the carpal tunnel fibroblasts contracting less at early time points (Fig. 2F). As differences in cell proliferation rates between the fibroblast cell lines may affect the contraction rate measured by FPCL, we assessed the cell proliferation rate of the cell lines with no differences observed (Fig. 2G).

To facilitate the standardization of future experiments, we assessed the usage of a commercially available neonatal fibroblast cell line in our *in vitro* study of *EPDR1* in Dupuytren. All three mRNA transcripts of *EPDR1* are expressed in the obtained neonatal fibroblast line PCS-201-010 (Fig. 3A and B). This cell line does not carry the susceptibility allele of rs16879765. In addition, these cells behave as expected in FPCL, as they contract the lattice without stimulation and contract faster upon TGF β 1 application (Fig. 3C). These results show that this commercially purchased fibroblast cell line derived from neonatal foreskin is suitable for *in vitro* analysis of *EPDR1* in on contractility.

To investigate the potential contribution of *EPDR1* to in myofibroblast contraction, we performed DsiRNA-mediated knockdown of *EPDR1* in PCS-201-010 fibroblasts. This approach resulted in a sustained and pronounced knockdown of *EPDR1* up to

at least 5 days post transfection, as determined by qPCR (Fig. 4A). Knockdown of *EPDR1* slowed the contraction rate in unstimulated FPCL conditions compared to controls (Fig. 4B), as well as upon TGF β 1 stimulation (Fig. 4C), although to a lesser extent. These results replicated. Cell proliferation was not significantly altered by *EPDR1* knockdown (Fig. 4D). These data imply a protective role of *EPDR1* knockdown in Dupuytren *in vitro*.

4. Discussion

With this work we identify a functional role of *EPDR1*, located within a recently discovered Dupuytren disease susceptibility locus [22,23]. The associated allele of SNP rs16879765, is more common in patients with Dupuytren disease than in controls [22]. Interestingly, the presence of this allele correlates with increased *EPDR1* expression in fibroblasts. Our results suggest that decreasing *EPDR1* expression in Dupuytren disease cells results in decreased collagen contraction, implying that *EPDR1* expression contributes to the well-established excessive collagen contractility of Dupuytren disease cells. This effect of *EPDR1* is not limited to Dupuytren disease cells, as it likely also affects contraction in healthy fibroblasts, such as the neonatal fibroblasts used in this study. Dupuytren disease is a contractile disease, so identifying novel genes that regulate collagen contraction may lead to novel

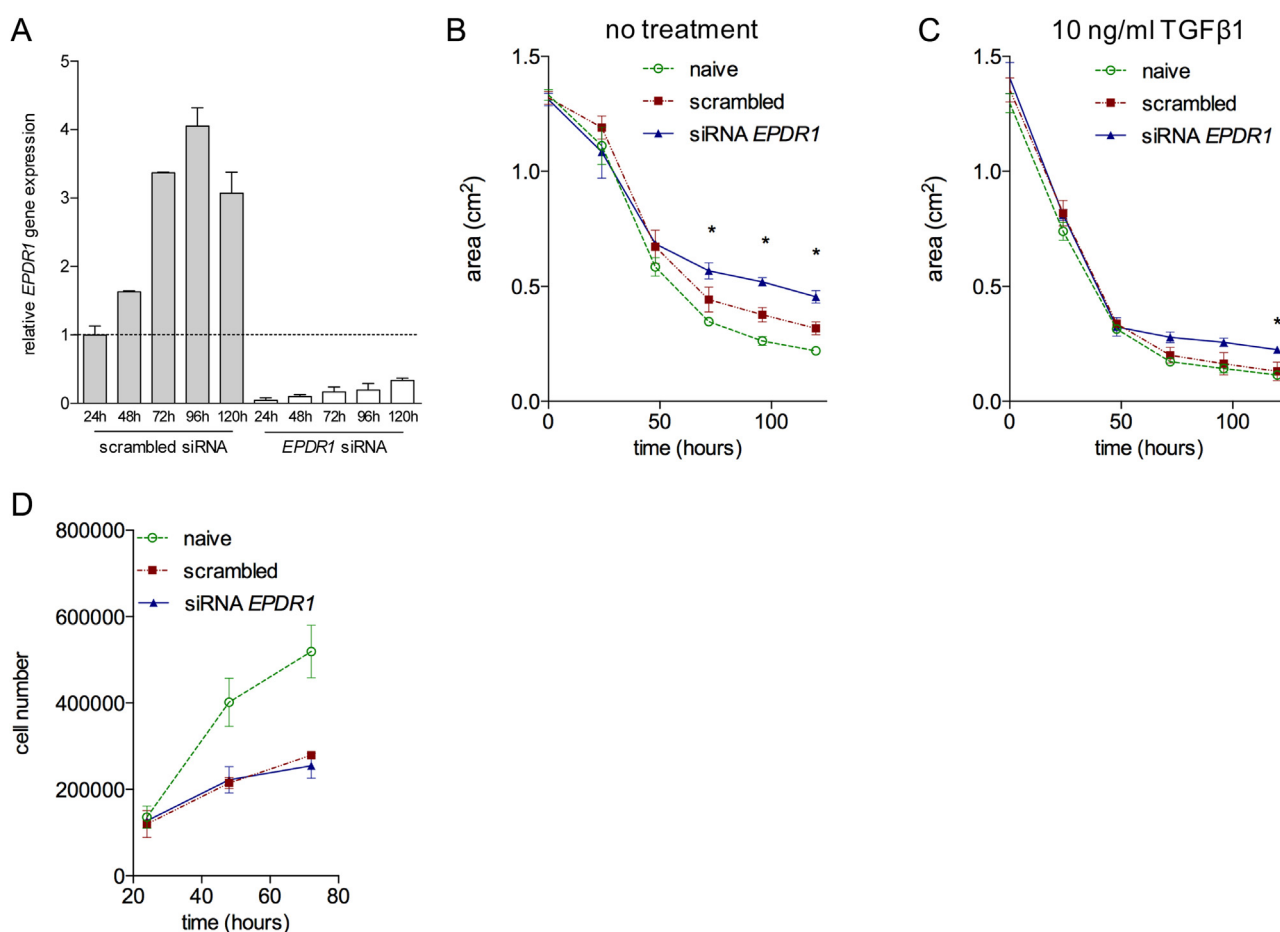


Fig. 4. *EPDR1* knockdown attenuates FPCL contractility. A. DsiRNA-mediated *EPDR1* knockdown assessed by qPCR. B. Contraction rate of PCS-201-010 treated with a scrambled dsiRNA (n = 3) or dsiRNA targeting *EPDR1* (n = 3; 2-way anova with repeated measures, Sidak post hoc analysis of means per treatment per time point, interaction effect p = 0.0008). Lattices with untreated cells were assessed to illustrate possible effects of transfection reagents upon FPCL, but were not included in the analysis. C. Contraction rate of PCS-201-010 treated with 10 ng/ml TGF β 1 and with a scrambled dsiRNA (n = 3) or dsiRNA targeting *EPDR1* (n = 3; 2-way anova with repeated measures, Sidak post hoc analysis of means per treatment per time point, interaction effect p = 0.03). Lattices with untreated cells were assessed to illustrate possible effects of transfection reagents upon FPCL, but were not included in the analysis. D. Cell proliferation rate of fibroblasts treated with a scrambled dsiRNA (n = 3) or dsiRNA targeting *EPDR1* (n = 3; 2-way anova with repeated measures, no significant effect). Untreated cells were assessed to illustrate possible effects of transfection reagents upon cell proliferation, but were not included in the analysis. Mean \pm standard deviation. *p < 0.05, **p < 0.01, ****p < 0.0001.

treatment approaches. Increase of EPDR1 levels is predicted to be one of many factors that enhance contractility in Dupuytren disease, but understanding the individual contributions of each potentially predisposing gene helps us to understand the pathogenesis of this disease.

The model employed to mimic Dupuytren *in vitro*, FPCL, has been used by others in the past. The validity of this model is based on the observation, from others and by us reported here, that fibroblasts from affected Dupuytren tissue contract faster than control tissue [16,19,35,36]. Here, we offer support that this model may be used for assessing the genetic contribution to Dupuytren pathophysiology by targeting gene expression of genes identified by genome-wide genetic studies. Despite this model's potential use in pharmacological screening, FPCL is naturally limited to mimicking Dupuytren *in vitro* and only in one cell type, hereby potentially excluding the effects of other non fibroblast-derived cells on Dupuytren onset and progression.

A contributing role of *EPDR1* in Dupuytren is not surprising, as extracellular matrix components are important in the fibromatosis [15,37,38] and ependymins have been previously associated with collagen [26,27]. The *EPDR1* gene produces 3 different transcripts all present in the fibroblasts we tested here. These transcripts translate to proteins harboring a transmembrane domain and/or ependymin domain. The association of ependymins to collagen was demonstrated in teleost fish where these secreted proteins bind to collagen [26,27]. In teleost fish their function was predicted to be anti-adhering and promoted learning and memory by (reviewed in [26]). Here, we propose a hypothesis that EPDR1 proteins containing a transmembrane domain and ependymin domain promote collagen adherence by binding collagen (with the ependymin domain) while remaining anchored to the cell (with the transmembrane domain). This hypothesis is supported by our data in which a knockdown of *EPDR1* results in a late and moderately attenuated contractility in FPCL [12]. This could explain the contraction conveyed by myofibroblasts in nodes on the cords leading to contractures in Dupuytren patients, although additional research is needed to understand the biomolecular intricacies of EPDR1 proteins in fibromatosis observed in Dupuytren.

In conclusion, here we show both genetic and biological evidence for a role of *EPDR1* in Dupuytren's contracture. Additionally, we demonstrate the applicability of the FPCL model to investigate genetic candidates in the disease. Future work may benefit incorporation a functional role for *EPDR1* in the development of therapeutic strategies for Dupuytren, as well as for other fibromatoses.

Conflict of interest

The authors have no conflict of interest to declare.

Acknowledgements

We thank Anil Ori and Tina Wang for helpful discussions and Yoon Jung for administrative support.

Appendix A. Supplementary data

Supplementary data associated with this article can be found, in the online version, at <http://dx.doi.org/10.1016/j.jdermsci.2016.04.015>.

References

- [1] K.G. Gudmundsson, T. Jonsson, R. Arngrimsson, Guillaume Dupuytren and finger contractures, *Lancet* 362 (2003) 165–168.

- [2] L.C. Hurst, M.A. Badalamente, V.R. Hentz, R.N. Hotchkiss, F.T. Kaplan, R.A. Meals, et al., Injectable collagenase clostridium histolyticum for Dupuytren's contracture, *N. Engl. J. Med.* 361 (2009) 968–979.
- [3] A.L. van Rijssen, P.M. Werker, Percutaneous needle fasciotomy in Dupuytren's disease, *J. Hand Surg. Br.* 31 (2006) 498–501.
- [4] D. Gilpin, S. Coleman, S. Hall, A. Houston, J. Karrasch, N. Jones, Injectable collagenase Clostridium histolyticum: a new nonsurgical treatment for Dupuytren's disease, *J. Hand Surg.* 35 (2027–2038) (2010) e2021.
- [5] J.R. Armstrong, J.S. Hurren, A.M. Logan, Dermofasciectomy in the management of Dupuytren's disease, *J. Bone Joint Surg. Br.* 82 (2000) 90–94.
- [6] J.J. Dias, J. Braybrooke, Dupuytren's contracture: an audit of the outcomes of surgery, *J. Hand Surg. Br.* 31 (2006) 514–521.
- [7] S. Hindocha, D.A. McGrouther, A. Bayat, Epidemiological evaluation of Dupuytren's disease incidence and prevalence rates in relation to etiology, *Hand (N Y)* 4 (2009) 256–269.
- [8] R. Lanting, E.R. van den Heuvel, B. Westerink, P.M. Werker, Prevalence of Dupuytren disease in The Netherlands, *Plast. Reconstr. Surg.* 132 (2013) 394–403.
- [9] S.G. Anthony, S.A. Lozano-Calderon, B.P. Simmons, J.B. Jupiter, Gender ratio of Dupuytren's disease in the modern U.S. population, *Hand (N Y)* 3 (2008) 87–90.
- [10] A.A. Khan, O.J. Rider, C.U. Jayadev, C. Heras-Palou, H. Giele, M. Goldacre, The role of manual occupation in the aetiology of Dupuytren's disease in men in England and Wales, *J. Hand Surg. Br.* 29 (2004) 12–14.
- [11] B. Shih, A. Bayat, Scientific understanding and clinical management of Dupuytren disease, *Nat. Rev. Rheumatol.* 6 (2010) 715–726.
- [12] J. Liu, Y. Wang, Q. Pan, Y. Su, Z. Zhang, J. et al. Han, Wnt/beta-catenin pathway forms a negative feedback loop during TGF-beta1 induced human normal skin fibroblast-to-myofibroblast transition, *J. Dermatol. Sci.* 65 (2012) 38–49.
- [13] L. Satish, P.H. Gallo, M.E. Baratz, S. Johnson, S. Kathju, Reversal of TGF-beta1 stimulation of alpha-smooth muscle actin and extracellular matrix components by cyclic AMP in Dupuytren's-derived fibroblasts, *BMC Musculoskelet. Disord.* 12 (2011) 113.
- [14] I. Ratkaj, M. Bujak, D. Jurisic, M. Bausloncar, K. Bendelja, K. Pavelic, et al., Microarray analysis of Dupuytren's disease cells: the profibrogenic role of the TGF-beta inducible p38 MAPK pathway, *Cell. Physiol. Biochem.* 30 (2012) 927–942.
- [15] W.L. Lam, J.M. Rawlins, R.O. Karoo, I. Naylor, D.T. Sharpe, Re-visiting Luck's classification: a histological analysis of Dupuytren's disease, *J. Hand Surg. Eur.* 35 (2010) 312–317.
- [16] L. Satish, D.B. O'Gorman, S. Johnson, C. Raykha, B.S. Gan, J.H. Wang, et al., Increased CCT-eta expression is a marker of latent and active disease and a modulator of fibroblast contractility in Dupuytren's contracture, *Cell Stress Chaperones* 18 (2013) 397–404.
- [17] J.M. Wilkinson, R.K. Davidson, T.E. Swingle, E.R. Jones, A.N. Corps, P. Johnston, et al., MMP-14 and MMP-2 are key metalloproteases in Dupuytren's disease fibroblast-mediated contraction, *Biochim. Biophys. Acta* 1822 (2012) 897–905.
- [18] I. Komatsu, J. Bond, A. Selim, J.J. Tomasek, L.S. Levin, H. Levinson, Dupuytren's fibroblast contractility by sphingosine-1-phosphate is mediated through non-muscle myosin II, *J. Hand Surg.* 35 (2010) 1580–1588.
- [19] R. Tse, J. Howard, Y. Wu, B.S. Gan, Enhanced Dupuytren's disease fibroblast populated collagen lattice contraction is independent of endogenous active TGF-beta2, *BMC Musculoskelet. Disord.* 5 (2004) 41.
- [20] L.S. Verjee, J.S. Verhoeckx, J.K. Chan, T. Krausgruber, V. Nicolaidou, D. Izadi, et al., Unraveling the signaling pathways promoting fibrosis in Dupuytren's disease reveals TNF as a therapeutic target, *Proc. Natl. Acad. Sci. U. S. A.* 110 (2013) E928–E937.
- [21] G.H. Dolmans, P.M. Werker, H.C. Hennies, D. Furniss, E.A. Festen, L. Franke, et al., Wnt signaling and Dupuytren's disease, *N. Engl. J. Med.* 365 (2011) 307–317.
- [22] G.H. Dolmans, P.M. Werker, H.C. Hennies, D. Furniss, E.A. Festen, L. Franke, et al., Wnt signaling and Dupuytren's disease, *N. Engl. J. Med.* 365 (2011) 307–317.
- [23] T. Debnjak, A. Zyluk, P. Puchalski, P. Serrano-Fernandez, Common variants of the EPDR1 gene and the risk of Dupuytren's disease, *Handchir. Mikrochir. Plast. Chir.* 45 (2013) 253–257.
- [24] V.E. Shashoua, Ependymin, a brain extracellular glycoprotein, and CNS plasticity, *Ann. N. Y. Acad. Sci.* 627 (1991) 94–114.
- [25] B. Ganss, W. Hoffmann, Calcium-induced conformational transition of trout ependymins monitored by tryptophan fluorescence, *Open Biochem. J.* 3 (2009) 14–17.
- [26] W. Hoffmann, H. Schwarz, Ependymins meningeal-derived extracellular matrix proteins at the blood-brain barrier, *Int. Rev. Cytol.* 165 (1996) 121–158.
- [27] H. Schwarz, A. Mullerschmid, W. Hoffmann, Ultrastructural-localization of ependymins in the endomeninx of the brain of the rainbow-trout – possible association with collagen fibrils of the extracellular-matrix, *Cell Tissue Res.* 273 (1993) 417–425.
- [28] I. Nimrich, S. Erdmann, U. Melchers, S. Chtarbova, U. Finke, S. Hentsch, et al., The novel ependymin related gene UCC1 is highly expressed in colorectal tumor cells, *Cancer Lett.* 165 (2001) 71–79.
- [29] C.C. Gregorio-King, J.L. McLeod, F.M. Collier, G.R. Collier, K.A. Bolton, G.J. Van Der Meer, et al., MERP1: a mammalian ependymin-related protein gene differentially expressed in hematopoietic cells, *Gene* 286 (2002) 249–257.
- [30] J. Apostolopoulos, R.L. Sparrow, J.L. McLeod, F.M. Collier, P.K. Darcy, H.R. Slater, et al., Identification and characterization of a novel family of mammalian

- ependymin-related proteins (MERPs) in hematopoietic, nonhematopoietic, and malignant tissues, *DNA Cell Biol.* 20 (2001) 625–635.
- [31] C. Raykha, J. Crawford, B.S. Gan, P. Fu, L.A. Bach, D.B. O’Gorman, IGF-II and IGFBP-6 regulate cellular contractility and proliferation in Dupuytren’s disease, *Biochim. Biophys. Acta* 1832 (2013) 1511–1519.
- [32] T.P. Yang, C. Beazley, S.B. Montgomery, A.S. Dimas, M. Gutierrez-Arcelus, B.E. Stranger, et al., Genevar: a database and Java application for the analysis and visualization of SNP-gene associations in eQTL studies, *Bioinformatics* 26 (2010) 2474–2476.
- [33] A.S. Dimas, S. Deutsch, B.E. Stranger, S.B. Montgomery, C. Borel, H. Attar-Cohen, et al., Common regulatory variation impacts gene expression in a cell type-dependent manner, *Science* 325 (2009) 1246–1250.
- [34] S.R. Walker, E.A. Nelson, D.A. Frank, STAT5 represses BCL6 expression by binding to a regulatory region frequently mutated in lymphomas, *Oncogene* 26 (2007) 224–233.
- [35] L. Satish, W.A. LaFramboise, S. Johnson, L. Vi, A. Njarlangattil, C. Raykha, et al., Fibroblasts from phenotypically normal palmar fascia exhibit molecular profiles highly similar to fibroblasts from active disease in Dupuytren’s Contracture, *BMC Med. Genomics* 5 (2012) 15.
- [36] M.A. Kuhn, X. Wang, W.G. Payne, F. Ko, M.C. Robson, Tamoxifen decreases fibroblast function and downregulates TGF(beta2) in Dupuytren’s affected palmar fascia, *J. Surg. Res.* 103 (2002) 146–152.
- [37] L. Satish, W.A. LaFramboise, D.B. O’Gorman, S. Johnson, B. Janto, B.S. Gan, et al., Identification of differentially expressed genes in fibroblasts derived from patients with Dupuytren’s Contracture, *BMC Med. Genomics* 1 (2008) 10.
- [38] L. Vi, A. Njarlangattil, Y. Wu, B.S. Gan, D.B. O’Gorman, Type-1 collagen differentially alters beta-catenin accumulation in primary Dupuytren’s Disease cord and adjacent palmar fascia cells, *BMC Musculoskelet Disord.* 10 (2009) 72.